Effects of the neutrino electromagnetic form factors on the neutrino and antineutrino mean free paths in dense matter

P.T.P. Hutauruk[a], A. Sulaksono[a] and T. Mart[a]

[a]Departemen Fisika, FMIPA, Universitas Indonesia, Depok, 16424, Indonesia

We have studied the effects of the nucleon weak magnetism and the neutrino electromagnetic properties on the neutrino and antineutrino mean free paths for all types of neutrinos. In the calculation, we consider matters with and without neutrino trapping as the target. We have found that the difference between the two mean free paths depends not only on the neutrino energy, but also on the matter density as well as matter constituents. Compared to the nucleon weak magnetism, the neutrino electromagnetic properties are found to have negligible effects on this difference.

1. Introduction

In the standard model, neutrinos have zero mass, magnetic moment, as well as electronic charge. However, there have been experimental upper limits on the electron-, muon- and tau-neutrino dipole moments given by $\mu_{\nu_e} < 1.5 \times 10^{-10}\mu_B$ [1] , $\mu_{\nu_\mu} < 7.4 \times 10^{-10}\mu_B$ [2] and $\mu_{\nu_\tau} < 5.4 \times 10^{-7}\mu_B$ [3], where μ_B is the Bohr magneton. While neutrino charge radii of $R = (0.54 \pm 0.82) \times 10^{-6}$ MeV^{-1} (for electron-neutrino) and $R < 0.40 \times 10^{-6}$ MeV^{-1} [4] (for muon-neutrino) have been experimentally evident, no experimental bound has been found so far on the charge radius of tau-neutrino [5]. On the other hand, the corresponding bounds from Super-K and SNO observations [5] are substantially larger, i.e., $\mu_{\nu_\tau}, \mu_{\nu_\mu} < 6.73\ (5.77) \times 10^{-10}\mu_B$ and $\mu_{\nu_e} < 6.45\ (5.65) \times 10^{-10}\mu_B$, whereas for the neutrino charge radii they obtained that $R_{\nu_\mu}, R_{\nu_\tau} < 2.31\ (1.98) \times 10^{-6}$ MeV^{-1} and $R_{\nu_e} < 1.33\ (1.16) \times 10^{-6}$ MeV^{-1}. Moreover, various astrophysical observations provide a limit on the neutrino magnetic moment in the range of $(1 - 4) \times 10^{-10}\mu_B$ [6], while from the plasmon decay in globular-cluster stars it is found that $\mu_\nu < 3 \times 10^{-12}\mu_B$ and $e_\nu < 2 \times 10^{-14}e$ [7], where e is the proton charge.

Using the standard neutrino properties, Horowitz and García [8] found that the muon-antineutrino mean free path in high density matter was considerably larger than the muon-neutrino one, provided that the weak magnetism of the nucleons is included. The sensitivity of differential cross section of the interaction between neutrinos and dense matter to the possibly nonzero neutrino electromagnetic properties has been also investigated [9, 10]. It is found that the effects of the neutrino electromagnetic properties on the differential cross section become more significant for the neutrino magnetic moment $\mu_\nu > 10^{-10}\mu_B$ and the neutrino charge radius $R > 10^{-5}$ MeV^{-1}. Motivated by this fact, in this paper we present the effect of the neutrino electromagnetic properties on the difference between neutrino and its antineutrino mean free paths. To this end, we follow the

same procedure as in Ref. [10], i.e., the differential cross section is calculated in a linear response with zero temperature approximation, while the leptons are assumed to be Fermi gas. In modeling the interacting nucleons, the relativistic mean field model inspired by effective field theory [11] has been used to describe the non strange dense matter with and without neutrino trapping.

2. Neutrino and antineutrino mean free paths

In this section we briefly discuss the analytic expression for the difference between neutrino-matter and antineutrino-matter cross sections. In this case the electromagnetic form factors of the neutrino-electron and the weak magnetism of the nucleons are taken into account. We start with the Lagrangian density of the neutrino-matter interactions for each constituent in the form of

$$\mathcal{L}^{j}_{\rm int} = \frac{G_F}{\sqrt{2}}\left(\bar{\nu}\Gamma^{\mu}_{\rm W}\nu\right)\left(\bar{\psi}J^{{\rm W}\ j}_{\mu}\psi\right) + \frac{4\pi\alpha}{q^2}\left(\bar{\nu}\Gamma^{\mu}_{\rm EM}\nu\right)\left(\bar{\psi}J^{{\rm EM}\ j}_{\mu}\psi\right), \tag{1}$$

where G_F and α are the coupling constant of the weak interaction and the electromagnetic fine structure constant, respectively, and $j = n, p, e^-, \mu^-$. The parity violating vertex of neutrinos is given by $\Gamma^{\mu}_{\rm W} = \gamma^{\mu}(1-\gamma^5)$, while the electromagnetic properties of Dirac neutrinos are described in terms of four form factors, i.e., $f_{1\nu}, g_{1\nu}, f_{2\nu}$ and $g_{2\nu}$, which stand for the Dirac, anapole, magnetic, and electric form factors, respectively. The electromagnetic vertex $\Gamma^{\mu}_{\rm EM}$ contains electromagnetic form factors [12, 13]. Explicitly, it reads

$$\Gamma^{\mu}_{\rm EM} = f_{m\nu}\gamma^{\mu} + g_{1\nu}\gamma^{\mu}\gamma^5 - (f_{2\nu} + ig_{2\nu}\gamma^5)\frac{P^{\mu}}{2m_e}, \tag{2}$$

where $f_{m\nu} = f_{1\nu} + (m_\nu/m_e)f_{2\nu}$, $P^{\mu} = k^{\mu} + k^{\mu\prime}$, m_ν and m_e are the neutrino and electron masses, respectively. In the static limit, the reduced Dirac form factor $f_{1\nu}$ and the neutrino anapole form factor $g_{1\nu}$ are related to the vector and axial-vector charge radii $\langle R^2_V\rangle$ and $\langle R^2_A\rangle$ through [12]

$$f_{1\nu}(q^2) = \tfrac{1}{6}\langle R^2_V\rangle q^2 \quad \text{and} \quad g_{1\nu}(q^2) = \tfrac{1}{6}\langle R^2_A\rangle q^2, \tag{3}$$

where the neutrino charge radius is defined by $R^2 = \langle R^2_V\rangle + \langle R^2_A\rangle$. In the limit of $q^2 \to 0$, $f_{2\nu}$ and $g_{2\nu}$ define the neutrino magnetic moment and the (CP violating) electric dipole moment, respectively [12, 14], i.e.,

$$\mu^m_\nu = f_{2\nu}(0)\mu_B \quad \text{and} \quad \mu^e_\nu = g_{2\nu}(0)\mu_B, \tag{4}$$

where μ^2_ν=$(\mu^m_\nu)^2$+ $(\mu^e_\nu)^2$. The explicit forms of $J^{{\rm W}\ j}_{\mu}$ [8] and $J^{{\rm EM}\ j}_{\mu}$ [15] are given by

$$J^{{\rm W}\ j}_{\mu} = F_1^{{\rm W}\ j}\gamma_\mu - G^j_A\gamma_\mu\gamma^5 + iF_2^{{\rm W}\ j}\ \frac{\sigma_{\mu\nu}q^\nu}{2M}, \qquad J^{{\rm EM}\ j}_{\mu} = F_1^{{\rm EM}\ j}\gamma_\mu + iF_2^{{\rm EM}\ j}\ \frac{\sigma_{\mu\nu}q^\nu}{2M}. \tag{5}$$

For antineutrinos, we must replace G^j_A with $-G^j_A$. In the limit of the photon point $q^2 \to 0$, for each type of neutrinos, the weak form factors $F^{\rm W}_1$, G_A and $F^{\rm W}_2$ are given in Table 1, whereas the electromagnetic form factors for each target $F^{\rm EM}_1$ and $F^{\rm EM}_2$ are shown in Table 2.

Table 1
Weak form factors in the limit of $q^2 \to 0$. Here we use $\sin^2\theta_{\rm w} = 0.231$, $g_A = 1.260$, $\mu_p = 1.793$ and $\mu_n = -1.913$ [8]. The index i indicates e, μ and τ.

Reaction	$F_1^{\rm W}$	G_A	$F_2^{\rm W}$
$\nu_i\ n \to \nu_i\ n$	-0.5	$-g_A/2$	$-(\mu_p-\mu_n)/2 - 2\sin^2\theta_{\rm w}\mu_n$
$\nu_i\ p \to \nu_i\ p$	$0.5 - 2\sin^2\theta_{\rm w}$	$g_A/2$	$(\mu_p-\mu_n)/2 - 2\sin^2\theta_{\rm w}\mu_p$
$\nu_e\ e \to \nu_e\ e$	$0.5 + 2\sin^2\theta_{\rm w}$	$1/2$	0
$\nu_\mu\ \mu \to \nu_\mu\ \mu$	$0.5 + 2\sin^2\theta_{\rm w}$	$1/2$	0
$\nu_{\mu,\tau}\ e \to \nu_{\mu,\tau}\ e$	$-0.5 + 2\sin^2\theta_{\rm w}$	$-1/2$	0
$\nu_{e,\tau}\ \mu \to \nu_{e,\tau}\ \mu$	$-0.5 + 2\sin^2\theta_{\rm w}$	$-1/2$	0

Table 2
Electromagnetic form factors of neutrinos in the limit of $q^2 \to 0$ [15].

Target	$F_1^{\rm EM}$	$F_2^{\rm EM}$
n	0	μ_n
p	1	μ_p
e	1	0
μ	1	0

Using the Lagrangian density given by Eq. (1), we can obtain the neutrino-matter and antineutrino-matter differential cross sections [10]. Their difference ($\Delta\sigma$) for each type of neutrino can be calculated from

$$\begin{aligned}\left[\frac{1}{V}\frac{d^3(\Delta\sigma)}{d^2\Omega d^2E'_\nu}\right]_i &= \sum_{j=p,n,e^-,\mu^-}\frac{1}{4\pi^2}\frac{E'_\nu}{E_\nu}\left[\left(\frac{G_F}{\sqrt{2}}\right)^2(2E-q_0)\left(F_1^{Wj}G_A^j + \frac{m}{M}F_2^{Wj}G_A^j\right)\Pi_{VA}^j\right. \\ &+ \left.\frac{8G_F\pi\alpha}{3\sqrt{2}}q^2R^2(2E-q_0)\left(\frac{m}{M}F_2^{EMj}G_A^j + F_1^{EMj}G_A^j\right)\Pi_{VA}^j\right], \qquad (6)\end{aligned}$$

where E_ν and E'_ν are the initial and final neutrino energies, respectively, while M is the target mass. For the nucleon m is the effective mass M^*, whereas for the lepton m=M. In Eq. (6) the charge radius of the neutrino is indicated by R. The explicit values of the target form factors F_i and G_A for each reaction are listed in Tables 1 and 2. The axial-vector polarization tensor Π_{VA} is given by

$$\Pi_{VA} = \frac{iq^2}{8\pi|\,\vec{q}\,|^3}\left[(E_F^2 - E^{*2}) + q_0(E_F - E^*)\right], \qquad (7)$$

where E_F and E^* denote the Fermi and effective energies of each target, respectively. From Eq. (6) it is obvious that, qualitatively, the charge radius of the neutrino yields some correction to the cross section difference, whereas this is not the case for the neutrino dipole moment. Its manifestation in the form of quantitative difference in the mean free path will be discussed in the following section.

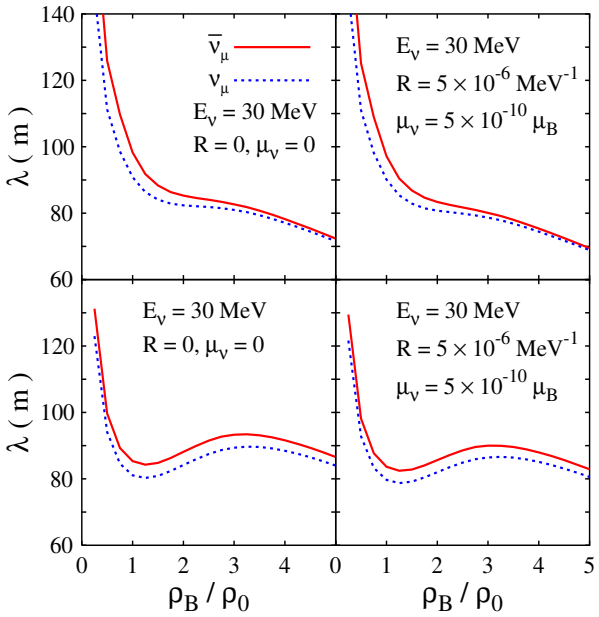

Figure 1. The muon-neutrino and muon-antineutrino mean free paths as a function of the ratio between nucleon and nuclear saturation densities. Results for the neutrinoless matter are shown in the upper panels, whereas results for the neutrino trapping with Y_{le}= 0.3 are shown in the lower panels.

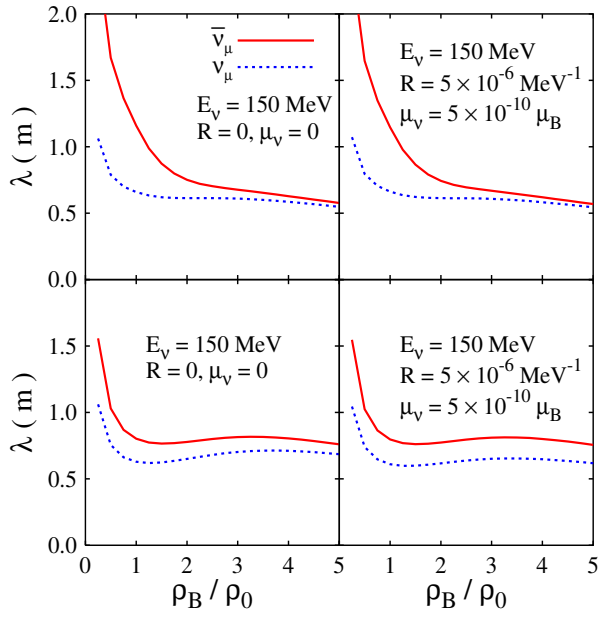

Figure 2. Same as Fig. 1, except with the muon-neutrino energy E_ν= 150 MeV.

3. Results and discussions

The neutrino and antineutrino mean free paths ($\lambda_{\nu,\ \bar{\nu}}$) as a function of the density at a certain neutrino energy is obtained by integrating the corresponding cross section over the time and vector components of the neutrino momentum transfer [8]. The λ_ν and $\lambda_{\bar{\nu}}$ for the case where the projectiles are electron-, muon-, tau-neutrinos, as well as their antineutrinos, are shown in Figs. 1, 2, 3 and 4. In this calculation we consider two types of matters, i.e., matters with and without neutrino trapping. In the latter, it is dominated by neutrons and followed by a small number of protons, electrons, and muons, which start to emerge at relatively large densities.

The existence of the neutrinos in matter also allows for the presence of a relatively large number of protons and electrons as compared to the case of neutrinoless matter. The appearance of these constituents is then followed by the appearance of a small number of muons at a density larger than twice of the nuclear saturation density. The relative fraction of the individual constituent of matter as a function of the ratio between nucleon and nuclear saturation densities can be found in Ref. [10]. In order to see the effect more clearly, in this calculation we use the relatively large values of neutrino dipole moments

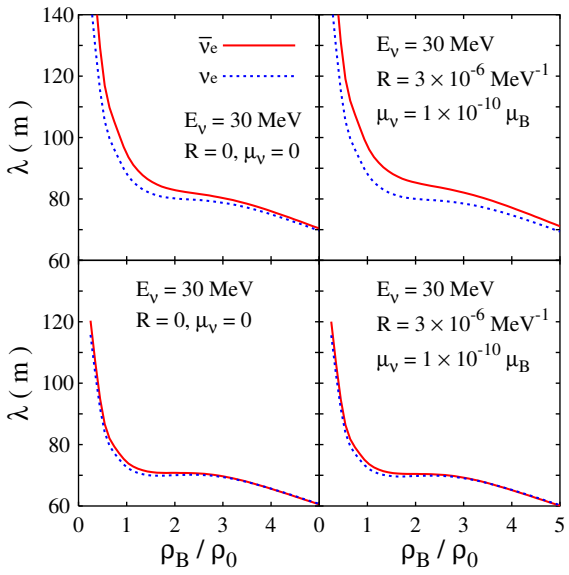

Figure 3. Same as Fig. 1, except for the electron-neutrino case.

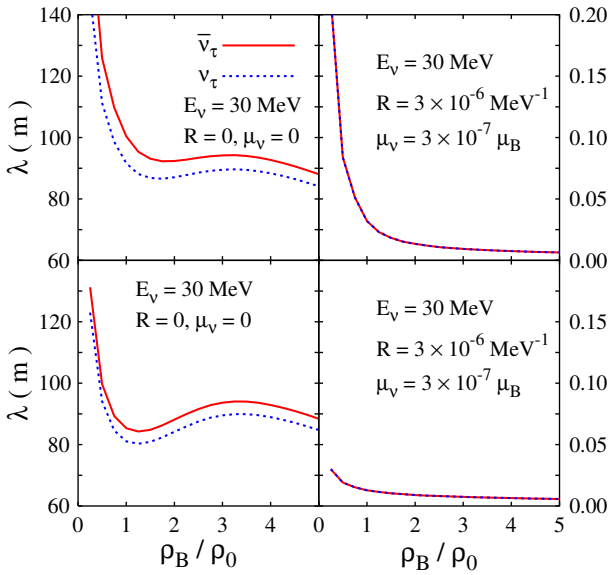

Figure 4. Same as Fig. 1, except for the tau-neutrino case.

and charge radii as compared to the stringent bounds.

In Fig. 1, it can be seen that in the case of matter without neutrino trapping, contribution of the neutrino charge radius is much smaller than that of the nucleon weak magnetism. Therefore, it does not give a visible effect in the difference between muon-neutrino and its antineutrino mean free paths. On the other hand, in the case of neutrino trapping, but with zero muon-neutrino dipole moment and charge radius, the difference is quite pronounced, especially at high densities. Albeit similar with the neutrinoless matter case, contribution from the neutrino charge radius is very small, and therefore it can not be observed within this kinematics. It is also apparent that in both cases of matter with densities around $(2-3)\rho_0$, λ_ν and $\lambda_{\bar{\nu}}$ behave differently, i.e., if neutrinos are present in the matter, the mean free paths increase with respect to the density, but if neutrinos are not present, the opposite phenomenon is observed.

For the case of neutrinoless matter, if the muon-neutrino energy is increased to 150 MeV (Fig. 2), the effect of the charge radius for this neutrino type can be neglected and the mean free path difference significantly increases at low densities. On the contrary, in the case of neutrino trapping, the mean free path difference appears to be more or less constant for all densities and a substantial enhancement caused by the neutrino charge radius contribution shows up only at high densities. As shown in Fig. 3, in spite of the fact that the effect is less significant in neutrinoless matter at high densities, contribution from the neutrino charge radius yields an enhancement to the difference between λ_ν and $\lambda_{\bar{\nu}}$. Interestingly, for the case of zero neutrino dipole moment and charge radius, but with neutrino trapping, the mean free path difference is suppressed. Thus, for this kind of matter, the effect of the neutrino charge radius in the mean free path difference is insignificant.

Similar to the muon-neutrino case, a different behavior of the mean free path is also observed in the tau-neutrino case at the densities around $(2-3)\rho_0$ (see Fig. 4). Due to the relatively large value of the tau-neutrino dipole moment used in this calculation, contribution from the protons to both mean free paths turns out to be very large and, as a consequence, the difference between λ_ν and $\lambda_{\bar{\nu}}$ is almost negligible.

4. Conclusions

We have calculated the neutrino and antineutrino mean free paths for all types of neutrinos and study their differences with various mechanisms, i.e., by using different types of matters (with and without neutrino trapping) as well as by including the weak magnetism of the nucleon and the electromagnetic form factors of the neutrinos. We have found that the difference in the neutrino and antineutrino mean free paths depends not only on the matter density, but also on the neutrino energy and the matter constituents. However, variation of the latter affects the mean free path difference in a distinct way. The effect of the neutrino electromagnetic form factors has been also studied. It is found that the corresponding contribution can be neglected as compared to the contribution from the nucleon weak magnetism.

Acknowledgment

AS and TM acknowledge the supports from the Faculty of Mathematics and Sciences, University of Indonesia, and from the Hibah Pascasarjana grant.

REFERENCES

1. J.F. Beacom and P. Vogel, Phys. Rev. Lett. 89 (1999) 5222.
2. D.A. Krakauer *et al.*, Phys. Lett. B 252 (1990) 177.
3. A.M Cooper-Sarkar *et al.*, Phys. Lett. B 280 (1992) 153.
4. P. Vilain *et al.*, Phys. Lett. B 345 (1995) 115.
5. A.S. Joshipura and S Mohanty, hep-ph/0108018 (2001).
6. Particle Data Group, K. Hagiwara *et al.*, Phys. Rev. D 66 (2002) 010001.
7. G.G. Raffelt, Phys. Rep. 320 (1999) 319.
8. C.J. Horowitz and M.A. Peréz-García, Phys. Rev. C 68 (2003) 025803.
9. C.K. Williams, P.T.P. Hutauruk, A. Sulaksono and T. Mart, Phys. Rev. D 71 (2005) 017303.
10. A. Sulaksono, C.K. Williams, P.T.P. Hutauruk, and T. Mart, Phys. Rev. C 73 (2006) 025803.
11. R.J. Furnstahl, B.D. Serot and H.B. Tang, Nucl. Phys. A 598 (1996) 539; Nucl. Phys. A 615 (1997) 441.
12. B.K. Kerimov, M. Ya Safin and H. Nazih, Izv. Akad. Nauk. SSSR Ser. Fiz. 52 (1998) 126.
13. A.M. Mourão, J. Pulido, and J.P. Ralston, Phys. Lett B 285 (1992) 364.
14. E. Nardi, AIP Conf. Proc. 670 (2003) 118.
15. P. Vogel and J. Engel, Phys. Rev. D 39 (1989) 3378.